A Balanced-to-Balanced Power Divider With Arbitrary Power Division

Bin Xia, Lin-Sheng Wu, *Member, IEEE*, Si-Wei Ren, and Jun-Fa Mao, *Fellow, IEEE*

***Abstract*—In this paper, a balanced-to-balanced power divider is proposed, for the first time, with arbitrary power division, which can be regarded as the balanced form of a Gysel power divider. The constraint rules are provided for its mixed-mode and single-ended S-parameters. The six-port network is analyzed by simplifying it to two-port networks with other ports matched at the central frequency. Its critical characteristic impedances are then calculated analytically by our derived equations according to the desired differential-mode power division ratio. The maximum achievable power division ratio is $1{:}4.69^2$ when the characteristic impedances are limited within the realizable range of 20–120 Ω. The impacts of several freely selected design parameters on the operating bandwidth are explored numerically. A prototype is realized by microstrip lines and lumped resistors with the power division ratio of $1{:}3^2$. The balanced-to-balanced performances of unequal power division, low differential-mode insertion loss, good suppression of common-mode noises, and mode conventions have been demonstrated by the simulated and measured results of the balanced-to-balanced power divider prototype.**

***Index Terms*—Arbitrary power division, balanced-to-balanced power divider/combiner, common mode, differential mode.**

I. Introduction

POWER dividers/combiners [1] are widely used to split or combine power or signals in various microwave and wireless communication systems, with specific performances of low insertion loss and high isolation between output ports. In many cases, power dividers are designed with equal power division to different outputs. However, in some cases, power dividers/combiners with unequal power division ratios are also desired, especially for feeding networks of antenna arrays. Single-ended power dividers with unequal power division have attracted much attention, due to their design flexibility for RF systems.

Manuscript received February 26, 2013; revised June 05, 2013; accepted June 10, 2013. Date of publication July 01, 2013; date of current version August 02, 2013. This work was supported by the National Basic Research Program of China under Grant 2009CB320202 and the National Natural Science Foundations of China under Grant 61234001 and Grant 61001014.

B. Xia is with the Key Lab of Ministry of Education for Design and Electromagnetic Compatibility of High-Speed Electronic Systems, Shanghai Jiao Tong University, Shanghai 200240, China, and also with the Zhenjiang Watercraft College People's Liberation Army (PLA), Zhenjiang City 212003, Jiangsu Province, China.

L.-S. Wu, S.-W. Ren, and J.-F. Mao are with the Key Lab of Ministry of Education for Design and Electromagnetic Compatibility of High-Speed Electronic Systems, Shanghai Jiao Tong University, Shanghai 200240, China (e-mail: jfmao@sjtu.edu.cn).

Color versions of one or more of the figures in this paper are available online at http://ieeexplore.ieee.org.

Digital Object Identifier 10.1109/TMTT.2013.2268739

According to the relationship between impedance ratio and power division ratio, different methods have been proposed to realize high-impedance transmission line for unequal power dividers. The defected ground structure [2], electromagnetic bandgap structure [3], swap structure of double-sided parallel-strip line (DSPSL) [4], offset DSPSL [5], coupled-line section with two shorted ends [6], and artificial transmission line loaded with opened and shorted stubs [7] were used for different power division ratios. In [8], the electrical lengths of line sections are adjusted to realize a power divider with very simple layout and unequal power division, and the impedance transformers at the two output ports are removed.

Multi-section topologies [9], [10] are used for wideband power dividers with unequal power division. A wideband Gysel divider was derived by replacing a 180° phase shifter with an ideal phase inverter in [11]. In [12] and [13], power dividers are designed for arbitrary real terminations and multiple ways, respectively, both with unequal power division. An unequal Wilkinson power divider with filtering response is proposed in [14]. Much research has been focused on dual-band power dividers with arbitrary power divisions more recently, in the forms of microstrip [15]–[19] and composite right-/left-handed transmission line [20].

On the other hand, balanced-to-balanced power dividers with common-mode suppression [21] are also desired now due to the increasing applications of balanced circuits and antennas in RF and microwave systems. In order to meet this technique demand, a Gysel and a Wilkinson balanced-to-balanced power divider are designed and implemented with a half-mode substrate integrated waveguide and microstrip line in our previous studies [22], [23], respectively. A simplified configuration is then proposed for the balanced-to-balanced form of the Wilkinson power divider to use only two lumped resistors [24]. In [25], an effective design method of balanced-to-balanced Wilkinson power divider is presented by converting its single-ended counterpart, and the number of resistors can be further reduced to one, at the cost of its operating bandwidth. By replacing the transmission lines with T-sections, a balanced-to-balanced power divider is implemented with a dual-band response [26]. However, all the proposed balanced-to-balanced power dividers are for equal power division. Arbitrary power division ratio has not been realized for the power dividers in the balanced form until now.

In this paper, a configuration of a balanced-to-balanced Gysel power divider with arbitrary power division is firstly proposed, and the design method is developed analytically. First, its corresponding constraint rules are summarized. Secondly, the design equations are derived for its critical characteristic impedances

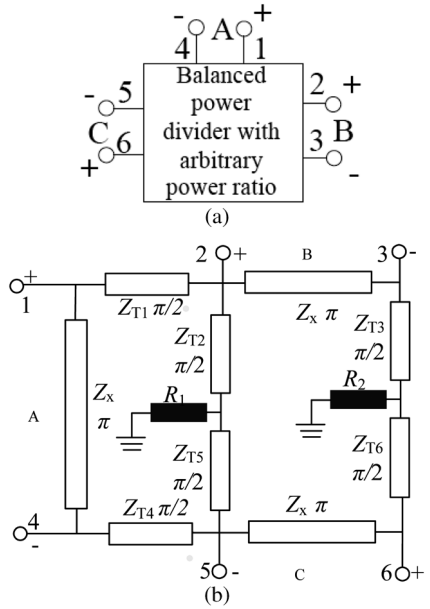

Fig. 1. Proposed balanced-to-balanced power divider with arbitrary power division. (a) Its diagram. (b) The structure.

and loaded resistances, by simplifying the six-port network to two-port networks with other ports matched. The realizable limitation of the power division ratio is predicted. Some special cases are then discussed. The relationship between its operating bandwidth and some design parameters is further explored. Finally, in order to validate our idea, a prototype is fabricated and measured. The experimental results agree well with the theoretical and simulated ones.

II. Constraint Rules of a Balanced-to-Balanced Power Divider With Arbitrary Power Division

The diagram of the proposed arbitrary balanced-to-balanced power divider is shown in Fig. 1(a). $[S^{\mathrm{std}}]$ represent its 6×6 scattering matrix. Assume it is a reciprocal six-port network, then we have $S_{mn} = S_{nm}$, where S_{mn} and S_{nm} are the elements of $[S^{\mathrm{std}}]$, and $m, n = 1, \ldots, 6$. The matrix is modified as

$$[S^{\mathrm{std\_}t}] = M^{-1}[S^{\mathrm{std}}]M = \begin{bmatrix} [S_{UL}] & [S_{UR}] \\ [S_{DL}] & [S_{DR}] \end{bmatrix} \tag{1}$$

where M is a transformation matrix. Its elements m_{ij} $(i, j = 1, \ldots, 6)$ are given by $m_{11} = m_{22} = m_{35} = m_{44} = m_{56} = m_{63} = 1$, and all the other elements are equal to 0. Note that the M matrix makes the single-ended ports in $[S^{\mathrm{std\_}t}]$ sorted as 1, 2, 6, 4, 3, and 5. The size of all the submatrices $[S_{UL}], [S_{UR}], [S_{DL}]$, and $[S_{DR}]$ of $[S^{\mathrm{std\_}t}]$ is 3×3. The four submatrices of the mixed-mode scattering matrix $[S^{mm}]$ are defined by

$$[S^{dd}] = \frac{1}{2}\{[S_{UL}] - [S_{UR}] - [S_{DL}] + [S_{DR}]\} \tag{2a}$$

$$[S^{dc}] = \frac{1}{2}\{[S_{UL}] + [S_{UR}] - [S_{DL}] - [S_{DR}]\} \tag{2b}$$

$$[S^{cd}] = \frac{1}{2}\{[S_{UL}] - [S_{UR}] + [S_{DL}] - [S_{DR}]\} \tag{2c}$$

$$[S^{cc}] = \frac{1}{2}\{[S_{UL}] + [S_{UR}] + [S_{DL}] + [S_{DR}]\}. \tag{2d}$$

The differential-mode input power should be divided with an arbitrary ratio, and the proposed component with arbitrary power division should satisfy the constraint rules in (3), shown at the bottom of this page, which is similar to those indicated in [23], where $0 < u < 1$ is the magnitude of $S_{dd\mathrm{AB}}$; φ_1, φ_2, φ_3, φ_4, and φ_5 are the undetermined phases of scattering parameters.

From (2) and (3), it can be derived that

$$\begin{aligned}[S_{UL}] &= \frac{1}{2}\{[S^{dd}] + [S^{dc}] + [S^{cd}] + [S^{cc}]\} \\ &= \begin{bmatrix} S_{11} & S_{12} & S_{16} \\ S_{21} & S_{22} & S_{26} \\ S_{61} & S_{62} & S_{66} \end{bmatrix} \\ &= \begin{bmatrix} \frac{1}{2}e^{j\varphi_3} & \frac{u}{2}e^{j\varphi_1} & \frac{\sqrt{1-u^2}}{2}e^{j\varphi_2} \\ \frac{u}{2}e^{j\varphi_1} & \frac{1}{2}e^{j\varphi_4} & 0 \\ \frac{\sqrt{1-u^2}}{2}e^{j\varphi_2} & 0 & \frac{1}{2}e^{j\varphi_4} \end{bmatrix} \end{aligned} \tag{4a}$$

$$\begin{aligned}[S_{UR}] &= \frac{1}{2}\{-[S^{dd}] + [S^{dc}] - [S^{cd}] + [S^{cc}]\} \\ &= \begin{bmatrix} S_{14} & S_{13} & S_{15} \\ S_{24} & S_{23} & S_{25} \\ S_{64} & S_{63} & S_{65} \end{bmatrix} \\ &= \begin{bmatrix} \frac{1}{2}e^{j\varphi_3} & -\frac{u}{2}e^{j\varphi_1} & -\frac{\sqrt{1-u^2}}{2}e^{j\varphi_2} \\ -\frac{u}{2}e^{j\varphi_1} & \frac{1}{2}e^{j\varphi_4} & 0 \\ -\frac{\sqrt{1-u^2}}{2}e^{j\varphi_2} & 0 & \frac{1}{2}e^{j\varphi_4} \end{bmatrix} \end{aligned} \tag{4b}$$

$$\begin{aligned}[S_{DL}] &= \frac{1}{2}\{-[S^{dd}] - [S^{dc}] + [S^{cd}] + [S^{cc}]\} \\ &= \begin{bmatrix} S_{41} & S_{42} & S_{46} \\ S_{31} & S_{32} & S_{36} \\ S_{51} & S_{52} & S_{56} \end{bmatrix} = [S_{UR}]^T \end{aligned} \tag{4c}$$

$$\begin{aligned}[S_{DR}] &= \frac{1}{2}\{[S^{dd}] - [S^{dc}] - [S^{cd}] + [S^{cc}]\} \\ &= \begin{bmatrix} S_{44} & S_{43} & S_{45} \\ S_{34} & S_{33} & S_{35} \\ S_{54} & S_{53} & S_{55} \end{bmatrix} = [S_{UL}]^T. \end{aligned} \tag{4d}$$

It should be pointed out that the constraint rules given by (4) can be directly used to design a balanced-to-balanced power

$$[S^{mm}] = \begin{bmatrix} [S^{dd}] & [S^{dc}] \\ [S^{cd}] & [S^{cc}] \end{bmatrix} = \begin{bmatrix} 0 & ue^{j\varphi_1} & \sqrt{1-u^2}e^{j\varphi_2} & 0 & 0 & 0 \\ ue^{j\varphi_1} & 0 & 0 & 0 & 0 & 0 \\ \sqrt{1-u^2}e^{j\varphi_2} & 0 & 0 & 0 & 0 & 0 \\ 0 & 0 & 0 & e^{j\varphi_3} & 0 & 0 \\ 0 & 0 & 0 & 0 & e^{j\varphi_4} & 0 \\ 0 & 0 & 0 & 0 & 0 & e^{j\varphi_5} \end{bmatrix} \tag{3}$$

divider with arbitrary power division, which are important to find a suitable structure and establish the design equations to determine its critical parameters.

III. Analysis and Design

A. Two-Port Network Between Ports 2 and 5 With Other Ports Matched

For the balanced-to-balanced power divider shown in Fig. 1(b), which can be regarded as a balanced-to-balanced Gysel power divider [23] with arbitrary power division, the two-port network between Ports 2 and 5 with other ports matched can be determined first. For simplification, the following analysis is only for the central frequency. According to (4), set the value of S_{22} and S_{55} to $-1/2$, i.e., $\varphi_4 = -\pi$, then the S-matrix $[S]_{25}$ of this two-port network is given by

$$[S]_{25} = \begin{bmatrix} S_{22} & S_{25} \\ S_{52} & S_{55} \end{bmatrix} = \begin{bmatrix} -\frac{1}{2} & 0 \\ 0 & -\frac{1}{2} \end{bmatrix}. \tag{5}$$

The Y-matrix is obtained as

$$[Y]_{25} = \begin{bmatrix} 3Y_0 & 0 \\ 0 & 3Y_0 \end{bmatrix} \tag{6}$$

where $Y_0 = 1/50\ \Omega^{-1}$ is the admittance of each port.

On the other hand, the Y-matrix of the two-port network can be calculated by

$$[Y]_{25} = [Y]_L + [Y]_M + [Y]_R \tag{7}$$

where $[Y]_L$, $[Y]_M$, and $[Y]_R$ are the Y-matrices of the left, middle, and right paths between Ports 2 and 5, respectively, as shown in Fig. 1(b). These three Y-matrices can be derived from their corresponding transfer matrices given in (8a)–(8c) at the bottom of this page. Note that the following transfer matrices in this section are derived for the two-port network between Ports 2 and 5 with the other ports matched. $[Y]_L$, $[Y]_M$, and $[Y]_R$ are then obtained by

$$[Y]_L = \begin{bmatrix} \frac{1}{2Z_{T1}^2 Y_0} & -\frac{1}{2Z_{T1}Z_{T4}Y_0} \\ -\frac{1}{2Z_{T1}Z_{T4}Y_0} & \frac{1}{2Z_{T4}^2 Y_0} \end{bmatrix} \tag{9a}$$

$$[Y]_M = \begin{bmatrix} \frac{R_1}{Z_{T2}^2} & \frac{R_1}{Z_{T2}Z_{T5}} \\ \frac{R_1}{Z_{T2}Z_{T5}} & \frac{R_1}{Z_{T5}^2} \end{bmatrix} \tag{9b}$$

$$[Y]_R = \begin{bmatrix} \frac{R_2}{Z_{T3}^2} + Y_0 & \frac{R_2}{Z_{T3}Z_{T6}} \\ \frac{R_2}{Z_{T3}Z_{T6}} & \frac{R_2}{Z_{T6}^2} + Y_0 \end{bmatrix}. \tag{9c}$$

Substituting (6) and (9) into (7), we have

$$\frac{R_1}{Z_{T2}^2} + \frac{R_2}{Z_{T3}^2} = 2Y_0 - \frac{1}{2Z_{T1}^2 Y_0} \tag{10a}$$

$$\frac{R_1}{Z_{T5}^2} + \frac{R_2}{Z_{T6}^2} = 2Y_0 - \frac{1}{2Z_{T4}^2 Y_0} \tag{10b}$$

$$\frac{R_1}{Z_{T2}Z_{T5}} + \frac{R_2}{Z_{T3}Z_{T6}} = \frac{1}{2Z_{T1}Z_{T4}Y_0}. \tag{10c}$$

B. Two-Port Network Between Ports 2 and 1 With Other Ports Matched

According to (4), S_{11} and S_{22} are set to $-1/2$ here, while S_{12} and S_{21} are set to $-ju/2$, which means $\varphi_1 = -\pi/2$ and $\varphi_3 = \varphi_4 = -\pi$. The S-matrix $[S]_{21}$ of the two-port network between Ports 2 and 1 with other ports matched then becomes

$$[S]_{21} = \begin{bmatrix} S_{22} & S_{21} \\ S_{12} & S_{11} \end{bmatrix} = \begin{bmatrix} -\frac{1}{2} & -j\frac{u}{2} \\ -j\frac{u}{2} & -\frac{1}{2} \end{bmatrix}. \tag{11}$$

The Y-matrix of this two-port network is transformed to be

$$[Y]_{21} = Y_0 \begin{bmatrix} \frac{3-u^2}{1+u^2} & j\frac{4u}{1+u^2} \\ j\frac{4u}{1+u^2} & \frac{3-u^2}{1+u^2} \end{bmatrix}. \tag{12}$$

On the other hand, the Y-matrix can be calculated by

$$[Y]_{21} = [Y]_{21R} + [Y]_{21L} \tag{13}$$

where $[Y]_{21R}$ is the Y-matrix of the quarter-wavelength transmission line between Ports 1 and 2, with the characteristic impedance of Z_{T1}, and is expressed by

$$[Y]_{21R} = \begin{bmatrix} 0 & j\frac{1}{Z_{T1}} \\ j\frac{1}{Z_{T1}} & 0 \end{bmatrix}. \tag{14}$$

$$\begin{aligned}[ABCD]_L &= \begin{bmatrix} 0 & jZ_{T1} \\ j\frac{1}{Z_{T1}} & 0 \end{bmatrix}\begin{bmatrix} 1 & 0 \\ Y_0 & 1 \end{bmatrix}\begin{bmatrix} -1 & 0 \\ 0 & -1 \end{bmatrix}\cdot\begin{bmatrix} 1 & 0 \\ Y_0 & 1 \end{bmatrix}\begin{bmatrix} 0 & jZ_{T4} \\ j\frac{1}{Z_{T4}} & 0 \end{bmatrix} \\ &= \begin{bmatrix} \frac{Z_{T1}}{Z_{T4}} & 2Z_{T1}Z_{T4}Y_0 \\ 0 & \frac{Z_{T4}}{Z_{T1}} \end{bmatrix}\end{aligned} \tag{8a}$$

$$\begin{aligned}[ABCD]_M &= \begin{bmatrix} 0 & jZ_{T2} \\ j\frac{1}{Z_{T2}} & 0 \end{bmatrix}\begin{bmatrix} 1 & 0 \\ \frac{1}{R_1} & 1 \end{bmatrix}\begin{bmatrix} 0 & jZ_{T5} \\ j\frac{1}{Z_{T5}} & 0 \end{bmatrix} \\ &= \begin{bmatrix} -\frac{Z_{T2}}{Z_{T5}} & -\frac{Z_{T2}Z_{T5}}{R_1} \\ 0 & -\frac{Z_{T5}}{Z_{T2}} \end{bmatrix}\end{aligned} \tag{8b}$$

$$\begin{aligned}[ABCD]_R &= \begin{bmatrix} -1 & 0 \\ 0 & -1 \end{bmatrix}\begin{bmatrix} 1 & 0 \\ Y_0 & 0 \end{bmatrix}\begin{bmatrix} 0 & jZ_{T3} \\ j\frac{1}{Z_{T3}} & 0 \end{bmatrix}\begin{bmatrix} 1 & 0 \\ \frac{1}{R_2} & 1 \end{bmatrix}\cdot\begin{bmatrix} 0 & jZ_{T6} \\ j\frac{1}{Z_{T6}} & 0 \end{bmatrix}\begin{bmatrix} 1 & 0 \\ Y_0 & 1 \end{bmatrix}\begin{bmatrix} -1 & 0 \\ 0 & -1 \end{bmatrix} \\ &= \begin{bmatrix} -\frac{Z_{T3}}{Z_{T6}} - Z_{\frac{T_3 Z_{T6} Y_0}{R_2}} & \frac{-Z_{T3}Z_{T6}}{R_2} \\ -\frac{Z_{T3}Y_0}{Z_{T6}} - \frac{Z_{T6}Y_0}{Z_{T3}} - \frac{Z_{T3}Z_{T6}Y_0^2}{R_2} & -\frac{Z_{T6}}{Z_{T3}} - \frac{Z_{T3}Z_{T6}Y_0}{R_2} \end{bmatrix}\end{aligned} \tag{8c}$$

$[Y]_{21L}$ is the Y-matrix of the other part of the two-port network between Ports 1 and 2, and can be transformed from its corresponding transfer matrix $[ABCD]_{21L}$, which is determined by

$$[ABCD]_{21L} = [ABCD]_{M+R} \begin{bmatrix} 1 & 0 \\ Y_0 & 1 \end{bmatrix} \begin{bmatrix} 1 & jZ_{T4} \\ j\frac{1}{Z_{T4}} & 0 \end{bmatrix} \cdot \begin{bmatrix} 1 & 0 \\ Y_0 & 1 \end{bmatrix} \begin{bmatrix} -1 & 0 \\ 0 & -1 \end{bmatrix} \quad (15)$$

where $[ABCD]_{M+R}$ is the transfer matrix of a part of the two-port network, which includes the middle and right paths between Ports 2 and 5, as indicated in Section III-A. It is derived from the Y-matrix $[Y]_{M+R}$, which can be determined by (6), (7), and (9a). We have

$$[Y]_{M+R} = [Y]_{25} - [Y]_L = \begin{bmatrix} 3Y_0 - \frac{1}{2Z_{T1}^2 Y_0} & \frac{1}{2Z_{T1}Z_{T4}Y_0} \\ \frac{1}{2Z_{T1}Z_{T4}Y_0} & 3Y_0 - \frac{1}{2Z_{T4}^2 Y_0} \end{bmatrix}. \quad (16)$$

$[ABCD]_{M+R}$ is then obtained as

$$[ABCD]_{M+R} = \begin{bmatrix} -6Z_{T1}Z_{T4}Y_0^2 + \frac{Z_{T1}}{Z_{T4}} & -2Z_{T1}Z_{T4}Y_0 \\ Z_{T1}Z_{T4}Y_0\left(\frac{3}{Z_{T1}^2} + \frac{3}{Z_{T4}^2} - 18Y_0^2\right) & -6Z_{T1}Z_{T4}Y_0^2 + \frac{Z_{T4}}{Z_{T1}} \end{bmatrix}. \quad (17)$$

According to (15) and (17), the following equations are derived:

$$[ABCD]_{21L} = \begin{bmatrix} A_{21L} & B_{21L} \\ C_{21L} & D_{21L} \end{bmatrix} \quad (18a)$$

$$A_{21L} = jZ_{T1}Z_{T4}^2 Y_0 \left(8Y_0^2 + \frac{1}{Z_{T4}^2}\right) \quad (18b)$$

$$B_{21L} = jZ_{T1}Z_{T4}^2 \left(8Y_0^2 - \frac{1}{Z_{T4}^2}\right) \quad (18c)$$

$$C_{21L} = jZ_{T1}Z_{T4}^2 Y_0^2 \left(24Y_0^2 - \frac{4}{Z_{T1}^2} + \frac{3}{Z_{T4}^2} - \frac{1}{Z_{T1}^2 Z_{T4}^2 Y_0^2}\right) \quad (18d)$$

$$= jZ_{T1}Z_{T4}^2 Y_0 \left(24Y_0^2 - \frac{4}{Z_{T1}^2} - \frac{3}{Z_{T4}^2}\right). \quad (18e)$$

According to (12), (13), and (14), $[Y]_{21L}$ can be rewritten as

$$[Y]_{21L} = \begin{bmatrix} \frac{3-u^2}{1+u^2}Y_0 & j\left(\frac{4uY_0}{1+u^2} - \frac{1}{Z_{T1}}\right) \\ j\left(\frac{4uY_0}{1+u^2} - \frac{1}{Z_{T1}}\right) & \frac{3-u^2}{1+u^2}Y_0 \end{bmatrix}. \quad (19)$$

Another form of $[ABCD]_{21L}$ can be transformed from (19), which is given by

$$A_{21L} = D_{21L} = j\frac{(3-u^2)Y_0 Z_{T1}}{4uY_0 Z_{T1} - 1 - u^2} \quad (20a)$$

$$B_{21L} = j\frac{(1+u^2)Z_{T1}}{4uY_0 Z_{T1} - 1 - u^2} \quad (20b)$$

$$C_{21L} = \frac{A_{21L}^2 - 1}{B_{21L}}. \quad (20c)$$

Due to $A_{21L} = D_{21L}$ in (20a), (18b) and (18e) lead to

$$\frac{1}{Z_{T1}^2} + \frac{1}{Z_{T4}^2} = 4Y_0^2. \quad (21)$$

Equation (18b) divided by (18c) should be equal to (20a) divided by (20b), i.e.,

$$Y_0 \frac{8Y_0^2 + 1/Z_{T4}^2}{8Y_0^2 - 1/Z_{T4}^2} = Y_0 \frac{3-u^2}{1+u^2}. \quad (22)$$

We then have

$$Z_{T4} = \frac{1}{2\sqrt{1-u^2}Y_0}. \quad (23)$$

Substituting (23) into (21), it is derived that

$$Z_{T1} = \frac{1}{2uY_0}. \quad (24)$$

If the ratio of the power that was divided to balanced port B and C is $1 : k^2$, the ratio of $|S_{dd\mathrm{AB}}|$ to $|S_{dd\mathrm{AC}}|$ is $1 : k$. From the constraint rules in (3), it is obtained that

$$\frac{|S_{dd\mathrm{AB}}|}{|S_{dd\mathrm{AC}}|} = \frac{u}{\sqrt{1-u^2}} = \frac{1}{k}. \quad (25)$$

We then have

$$u = \frac{1}{\sqrt{1+k^2}}. \quad (26)$$

Substituting (26) into (23) and (24), the following equations are obtained:

$$Z_{T1} = \frac{1}{2Y_0}\sqrt{1+k^2} \quad (27a)$$

$$Z_{T4} = \frac{1}{2Y_0}\sqrt{1+\frac{1}{k^2}} \quad (27b)$$

$$\frac{Z_{T1}}{Z_{T4}} = k. \quad (27c)$$

If Z_{T1}, Z_{T4}, and u are replaced with (27a), (27b), and (26), respectively, we can find that the transfer parameters of (18) have the same values as those of (20).

C. Design Freedom and Limitation

From (10) and (27), the following equations are obtained:

$$\frac{R_1}{Z_{T2}^2} + \frac{R_2}{Z_{T3}^2} = 2Y_0 \frac{k^2}{1+k^2} \quad (28a)$$

$$\frac{R_1}{Z_{T5}^2} + \frac{R_2}{Z_{T6}^2} = 2Y_0 \frac{1}{1+k^2} \quad (28b)$$

$$\frac{R_1}{Z_{T2}Z_{T5}} + \frac{R_2}{Z_{T3}Z_{T6}} = 2Y_0 \frac{k}{1+k^2}. \quad (28c)$$

We can further derive that

$$Z_{T2} = \sqrt{\frac{(R_1 + R_2/a^2)(1+1/k^2)}{2Y_0}} \quad (29a)$$

$$Z_{T3} = aZ_{T2} = \sqrt{\frac{(a^2R_1 + R_2)(1+1/k^2)}{2Y_0}} \quad (29b)$$

$$Z_{T5} = kZ_{T2} = \sqrt{\frac{(R_1 + R_2/a^2)(1+k^2)}{2Y_0}} \quad (29c)$$

$$Z_{T6} = akZ_{T2} = \sqrt{\frac{(a^2R_1 + R_2)(1+k^2)}{2Y_0}} \quad (29d)$$

where a is the impedance ratio of Z_{T3} to Z_{T2}. We then set

$$R_{1c} = \frac{(R_1 + R_2/a^2)}{2} \tag{30a}$$

$$R_{2c} = \frac{(a^2 R_1 + R_2)}{2} \tag{30b}$$

$$m = \frac{R_2}{R_{2c}} = \frac{2R_2}{a^2 R_1 + R_2}. \tag{30c}$$

Equation (30) means

$$R_1 = (2 - m)R_{1c} \tag{31a}$$

$$R_2 = mR_{2c}. \tag{31b}$$

From (31), it is seen that the coefficient m should be selected within $[0, 2]$ to guarantee R_1 and R_2 are always non-negative. Equation (29) is then rewritten as

$$Z_{T2} = \sqrt{\frac{R_{1c}(1 + 1/k^2)}{Y_0}} = \frac{Z_{T5}}{k} \tag{32a}$$

$$Z_{T3} = \sqrt{\frac{R_{2c}(1 + 1/k^2)}{Y_0}} = \frac{Z_{T6}}{k}. \tag{32b}$$

The values of R_{1c} and R_{2c} can also be selected arbitrarily, but note that Z_{T2}, Z_{T3}, Z_{T5}, and Z_{T6} should all have realizable values when selecting m, R_{1c}, and R_{2c}. Assuming $k \geq 1$ without loss of generality, we will have

$$Z_L \leq \sqrt{\frac{R_{ic}(1 + 1/k^2)}{Y_0}} \tag{33a}$$

$$\sqrt{\frac{R_{ic}(1 + k^2)}{Y_0}} \leq Z_H \tag{33b}$$

where $i = 1$ and 2, Z_L, and Z_H are the lower and upper limits of realizable characteristic impedances of transmission lines, respectively. Combining (33a) and (33b), it is derived that

$$\frac{Z_L^2 Y_0}{1 + 1/k^2} = R_{\min} \leq R_{1c}, R_{2c} \leq R_{\max} = \frac{Z_H^2 Y_0}{1 + k^2} \tag{34}$$

where $R_{\min}$ and $R_{\max}$ are the minimum and maximum realizable values for R_{1c} (also for R_{2c}), respectively. It is found from (34) that

$$k \leq \frac{Z_H}{Z_L}. \tag{35}$$

Since the condition of $Z_L \leq 1/(2Y_0)$ can easily be achieved, it is derived from (27a) that

$$k \leq \sqrt{(2Z_H Y_0)^2 - 1} \leq \frac{Z_H}{Z_L}. \tag{36}$$

Equation (36) is the realizable limitation of the division ratio k. If $Y_0 = 1/50\ \Omega^{-1}$, $Z_L = 20\ \Omega$, and $Z_H = 120\ \Omega$, the maximum realizable division ratio is $k = 4.69$. If $k = 3$ is desired, the values of R_{1c} and R_{2c} should be within $[7.2, 28.8]$, while the values of R_1 and R_2 should be within $[0, 57.6]$.

When $R_{1c} = R_{2c}$, we will have

$$Z_{T2} = Z_{T3} = \sqrt{\frac{R_{1c}(1 + 1/k^2)}{Y_0}} = \frac{Z_{T5}}{k} = \frac{Z_{T6}}{k}. \tag{37}$$

The transmission lines in the two paths between balanced ports B and C will then have the same characteristic impedances. Note that even in this case, the values of R_1 and R_2 can still be different from each other with $m \neq 1$. If $R_1 = R_2$ is also satisfied, (37) can be further simplified as

$$Z_{T2} = Z_{T3} = \sqrt{\frac{R_1(1 + 1/k^2)}{Y_0}} = \frac{Z_{T5}}{k} = \frac{Z_{T6}}{k}. \tag{38}$$

When $R_{1c} \to +\infty$, we have $Z_{T2} \to +\infty$, $Z_{T5} \to +\infty$, and $R_1 \to +\infty$. The value of $a = Z_{T3}/Z_{T2}$ is close to 0, leading to $m = 2$ from (30c). It can then be derived from (29b) and (29d) that

$$Z_{T3} = \sqrt{\frac{R_2(1 + 1/k^2)}{(2Y_0)}} = \frac{Z_{T6}}{k}. \tag{39}$$

In this special case, the $Z_{T2} - R_1 - Z_{T5}$ path between Ports 2 and 5 is dismissed, and only one resistor of R_2 is required. When selecting the value of R_2, Z_{T3} and Z_{T6} should still be within the realizable range of characteristic impedance. We then have

$$\frac{2Z_L^2 Y_0}{1 + 1/k^2} \leq R_2 \leq \frac{2Z_H^2 Y_0}{1 + k^2}. \tag{40}$$

If $Y_0 = 1/50\ \Omega^{-1}$, $Z_L = 20\ \Omega$, $Z_H = 120\ \Omega$, and $k = 3$, the value of R_2 should be within $[14.4, 57.6]$. A similar conclusion can also be drawn from the case of $R_{2c} \to +\infty$.

We can also find that the proposed balanced-to-balanced power divider with arbitrary power division can be built with only one resistor when $R_1 = 0\ \Omega$ or $R_2 = 0\ \Omega$ corresponding to $m = 2$ or 0, respectively. In these cases, another position for the loading resistor is replaced by a shorted end.

Note that the proposed balanced-to-balanced Gysel power divider with an arbitrary power division ratio has a good power-handling capability since the isolation resistors are shunted to the ground, and the resistors are easily replaced by high-power loads. The power-handling capability limited by the microstrip lines is usually much larger than that limited by the resistors or loads.

D. Bandwidth With Different Values of m, k, R_{1c}, and R_{2c}

Although the above analysis is only for the central frequency, the proposed component can be used within a specific operating

band. According to our previous work [23], when the characteristic impedance Z_x of half-wavelength transmission lines, which are regarded as phase inverters at the central frequency, is set to 50 Ω, the operating fractional bandwidth (FBW) will be relatively wide. If the values of $|S_{dd\mathrm{AB}}|$, $|S_{dd\mathrm{AC}}|$, $|S_{cc\mathrm{AA}}|$, $|S_{cc\mathrm{BB}}|$, and $|S_{cc\mathrm{CC}}|$ are better than -1 dB from their maximum magnitudes and the values of $|S_{dd\mathrm{AA}}|$, $|S_{dd\mathrm{BB}}|$, $|S_{dd\mathrm{CC}}|$, $|S_{dd\mathrm{BC}}|$, $|S_{cc\mathrm{AB}}|$, $|S_{cc\mathrm{AC}}|$, $|S_{cc\mathrm{BC}}|$, $|S_{dc\mathrm{AA}}|$, $|S_{dc\mathrm{AB}}|$, $|S_{dc\mathrm{AC}}|$, $|S_{dc\mathrm{BB}}|$, $|S_{dc\mathrm{BA}}|$, $|S_{dc\mathrm{BC}}|$, $|S_{dc\mathrm{CC}}|$, $|S_{dc\mathrm{CA}}|$, and $|S_{dc\mathrm{CB}}|$ all below -15 dB should be satisfied simultaneously, an operating band can be measured, which is denoted by BW.S.

If the values of the phase difference between $S_{dd\mathrm{AB}}$ and $S_{dd\mathrm{AC}}$ is below 10° should be satisfied, an operating band related phase can be determined. We define BW.P as the bandwidth determined by 10° phase difference. From Fig. 2, with the constants of $m = 1$ and $R_{1c} = R_{1c} = 18\ \Omega$, it is found that the FBW decreases with the increasing of k. Comparing with FBW.S with FBW.P, we find FBW.P in Fig. 3 is larger than FBW.S in the theoretical results.

Here, the relationship between FBW and the values of design parameters m, R_{1c}, and R_{2c} is explored numerically for some typical cases.

From Fig. 2(a), it is found that the FBW of the proposed power divider is influenced by m and the maximum bandwidth for a certain m decreases with the increasing of k. The simplified structure only with R_1 or R_2 has narrower bandwidth than the structure in Fig. 1(b), and the theoretical results can be seen from Fig. 2(b)–(d) for $k = 1, 2$, and 3. The theoretical result has wider bandwidth than its related measured results.

From Fig. 2(a), it is found that the FBW of the proposed power divider is influenced by m and the maximum bandwidth for a certain m decreases with the increasing of k. With constant $m = 1$ and $k = 3$, the theoretical FBW will increase with both R_{1c} and R_{2c}, as shown in Fig. 2(b). When the values of R_{1c} and R_{2c} are both larger than 20 Ω, the FBW is almost unchanged with the resistance parameters.

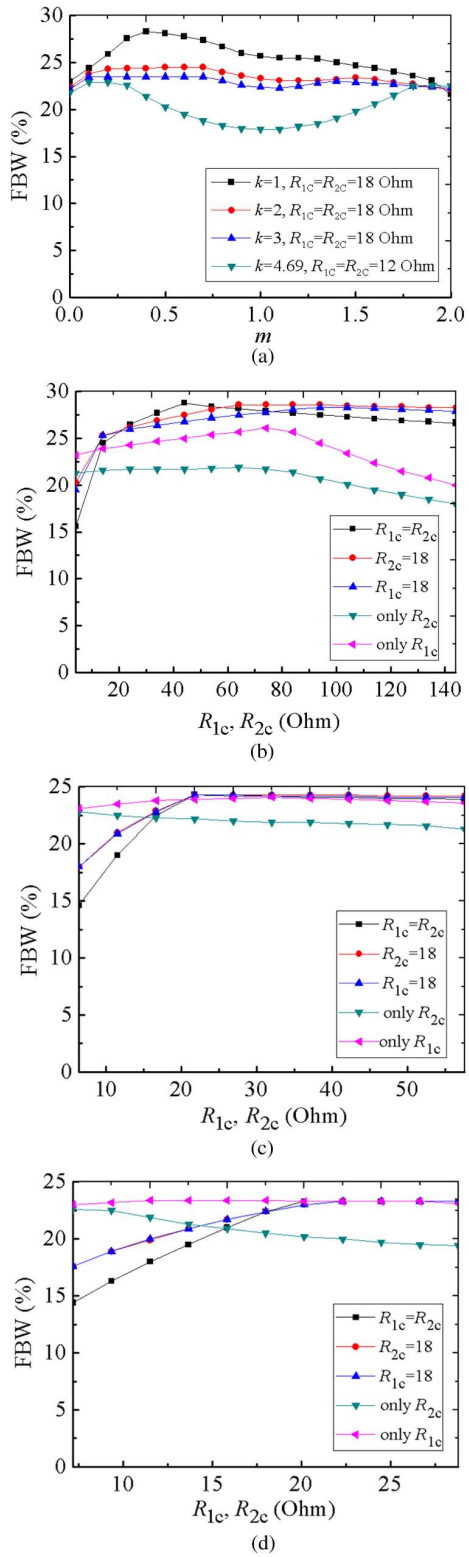

Fig. 2. FBW of the proposed balanced-to-balanced power divider: (a) for $k = 1$ and 3 when $R_{1c} = R_{2c} = 18\ \Omega$, and for $k = 4.69$ when $R_{1c} = R_{2c} = 12\ \Omega$ with m changed. (b) $k = 1$, $m = 1$, for different values of R_{1c}, R_{2c} when $R_{1c} = R_{1c}$; for different values of R_{2c} when $R_{1c} = 18\ \Omega$, and for different values of R_{1c} when $R_{2c} = 18\ \Omega$; for different values of R_{2c} when $R_{1c} = 18\ \Omega$, and for different values of R_{1c} when $R_{2c} = 18\ \Omega$; for different values of R_{2c} when the $Z_{T2} - R_1 - Z_{T5}$ path between Ports 2 and 5 is dismissed; for different values of R_{1c} when the $Z_{T3} - R_2 - Z_{T6}$ path between Ports 3 and 6 is dismissed; (c) $k = 2$; (d) $k = 3$. The curves in (c) and (d) are described as (b).

IV. Results and Discussion

A. Design Procedure

Based on our method, we can design a balanced-to-balanced power divider by the following procedure.

Step 1) From the designed power ratio, we can get Z_{T1}, Z_{T4}.

Step 2) Tuning m, R_{1c}, R_{2c}, we can get maximum FBW curves.

Step 3) From determined m, R_{1c}, R_{2c}, we can get $Z_{T2}, Z_{T3}, Z_{T5}, Z_{T6}, R_1, R_2$. R_1, R_2 must be commercially available, Z_{T1}–Z_{T6} must be in the range of Z_L and Z_H.

Step 4) Considering the discontinuities, via, loss, and dispersion of substrate in the simulation and fabrication.

B. Theoretical Results

A balanced-to-balanced power divider prototype is developed with the power division ratio between balanced B and C of 1:3[2]. The design parameters are chosen as $m = 1$, $R_{1c} = R_{2c} = 25\ \Omega$, and $Z_x = 50\ \Omega$. The other critical characteristic impedances and loaded resistances are calculated by (19), (23), and (24), which are

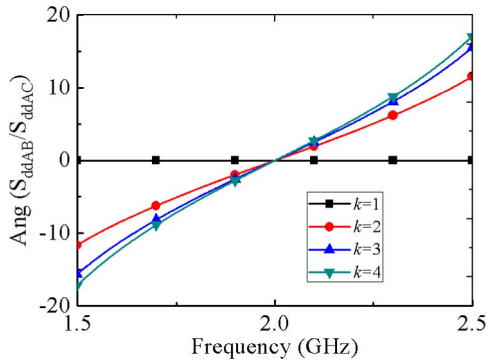

Fig. 3. Phase differences between $S_{dd\mathrm{AB}}$ and $S_{dd\mathrm{AC}}$, when $R_{1c} = R_{2c} = 16\ \Omega$ and $m = 1$.

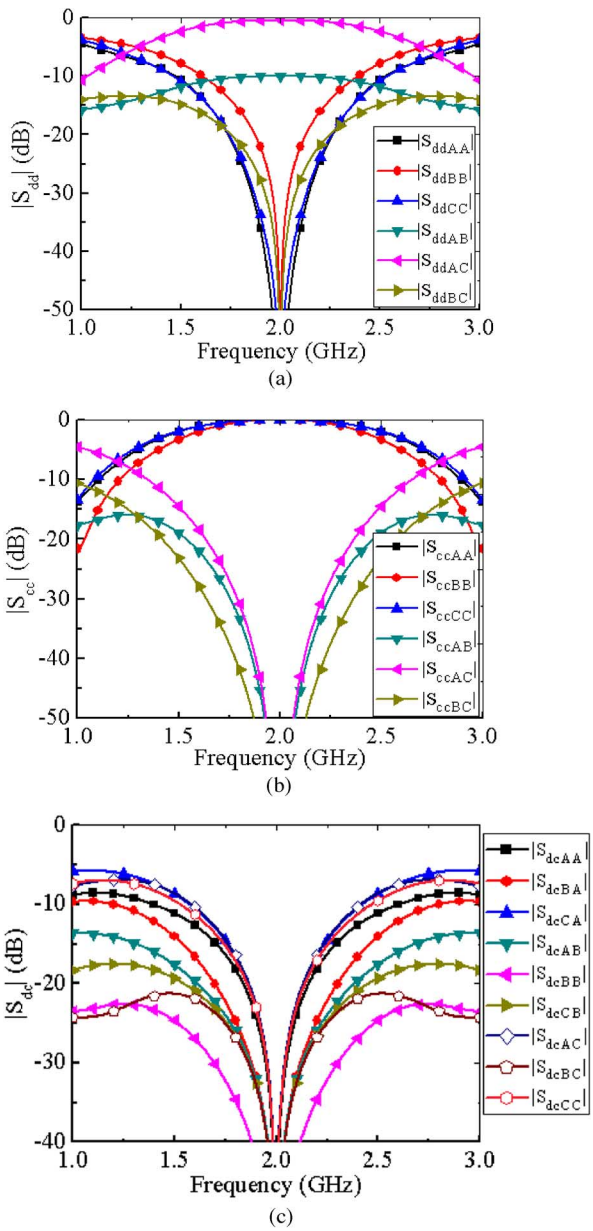

Fig. 4. Theoretical mixed-mode S-parameters of the proposed balanced-to-balanced power divider prototype with power division ratio of 1:3[2]. (a) S_{dd}. (b) S_{cc}. (c) S_{dc}.

$Z_{T1} = 79.06\ \Omega$, $Z_{T2} = Z_{T3} = 37.27\ \Omega$, $Z_{T4} = 26.35\ \Omega$, $Z_{T5} = Z_{T6} = 111.8\ \Omega$, and $R_1 = R_2 = 25\ \Omega$.

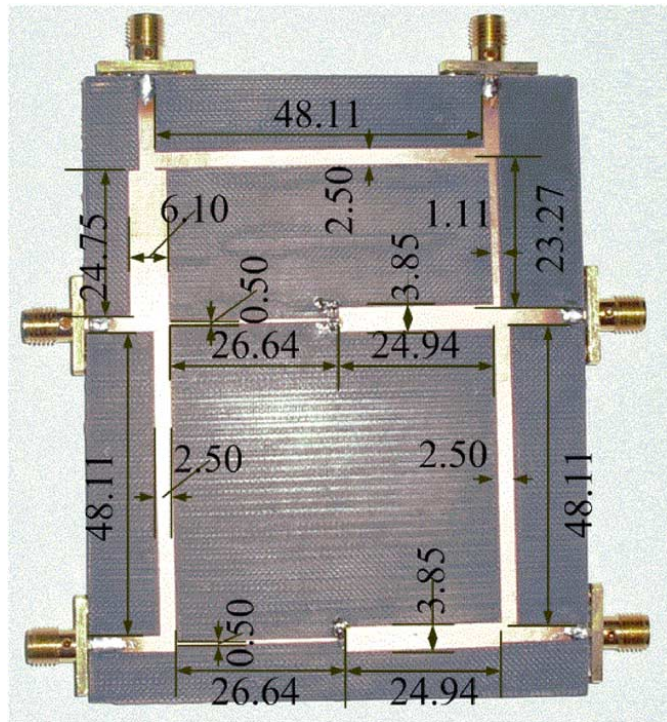

Fig. 5. Photograph of the fabricated prototype of the proposed balanced-to-balanced power divider with arbitrary power division.

From (1), we have

$$\left[S_{3\times3}^{cd}\right] = \left[S_{3\times3}^{dc}\right]^{T}. \tag{41}$$

The two matrices $[S^{dc}]$ and $[S^{cd}]$ have been defined in [23]. The theoretical results of the equivalent-circuit model in Fig. 1(b) are plotted in Fig. 4. The differential-mode transmission coefficient and the common-mode reflection coefficient reach their maximum of $|S_{dd\mathrm{AB}}| = -10$ dB, $|S_{dd\mathrm{AC}}| = -0.46$ dB, and $|S_{cc\mathrm{AA}}| = |S_{cc\mathrm{BB}}| = |S_{cc\mathrm{CC}}| = 0$ dB at $f_0 = 2.0$ GHz, respectively. An operating band determined by mixed-mode S-parameters is 1.77 to 2.23 GHz, i.e., the FBW is about 23%.

C. Simulated and Measured Results

As shown in Fig. 5, the prototype is fabricated on an F4B substrate with the relative permittivity of $\varepsilon_r = 2.65$, the loss tangent of $\tan\delta = 0.003$, and the thicknesses of $h = 0.73$ mm. The balanced-to-balanced power divider occupies an area of about $0.5 \times 0.75\lambda_g^2$, where λ_g is the guided wavelength at the central frequency.

Fig. 6(a) and (b) shows a comparison between the simulated and measured transmission coefficients, reflection coefficients, and isolation between balanced ports B and C for differential- and common-mode operations, respectively. Fig. 6(c) and (d) provides a comparison between the simulated and measured differential-to-common mode conversions. The curves of $|S_{dd\mathrm{AB}}|$, $|S_{dd\mathrm{AC}}|$, $|S_{cc\mathrm{AA}}|$, $|S_{cc\mathrm{BB}}|$, and $|S_{cc\mathrm{CC}}|$ are magnified in Fig. 6(e).

The theoretical maximum differential-mode transmission coefficients of the prototype are $|S_{dd\mathrm{AB}}| = -10$ dB and $|S_{dd\mathrm{AC}}| = -0.46$ dB at the central frequency of 2 GHz. In

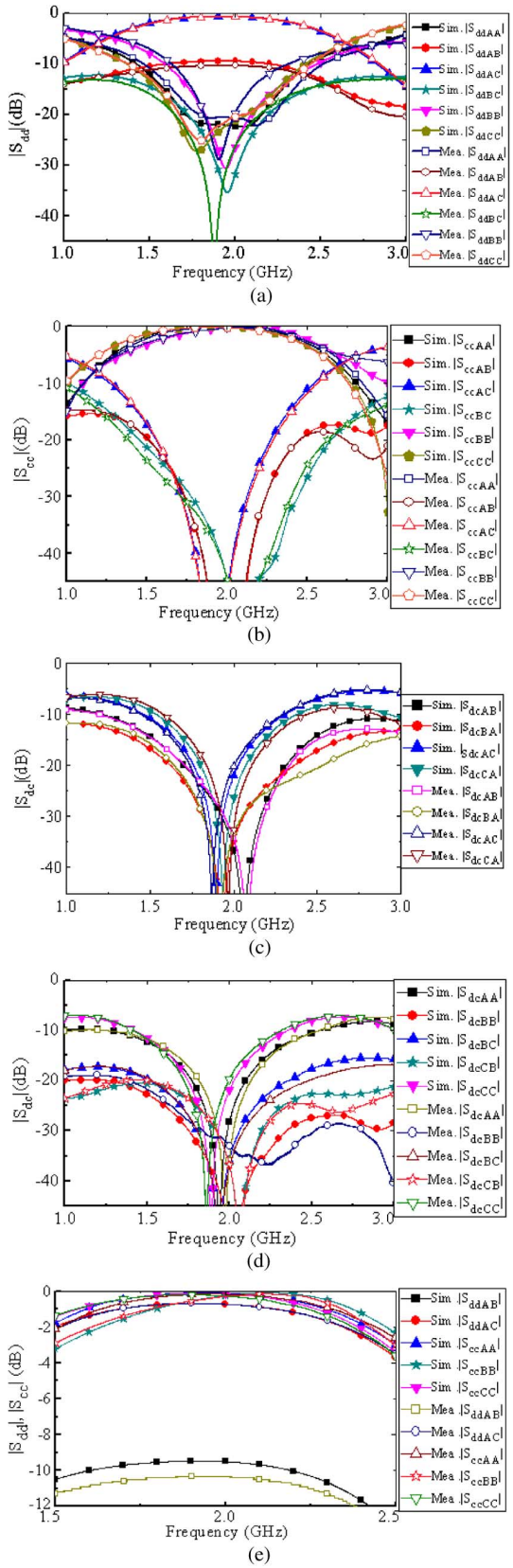

Fig. 6. Simulated and measured mixed-mode S-parameters of the proposed balanced-to-balanced power divider prototype with power division ratio of 1:3[2]. (a) S_{dd}. (b) S_{cc}. (c) and (d) S_{dc}. (e) Magnified curves of $|S_{ddAB}|$, $|S_{ddAC}|$, $|S_{ccAA}|$, $|S_{ccBB}|$, and $|S_{ccCC}|$. Mea. and Sim. represent the measured and simulated results, respectively.

the measurements, the maximum differential-mode transmission coefficient of the prototype is $|S_{ddAB}| = -10.32$ dB at 1.96 GHz, $|S_{ddAC}| = -0.94$ dB at 1.95 GHz, the best differential-mode isolation is 61.72 dB at 1.88 GHz, and the common-mode reflection coefficients of $|S_{ccAA}|$ and $|S_{ccBB}|$ reach their maximum of -0.16 and -0.2 dB at 2.11 and 2.06 GHz, respectively. The conversions between differential- and common-mode signals are successfully suppressed around the central frequency.

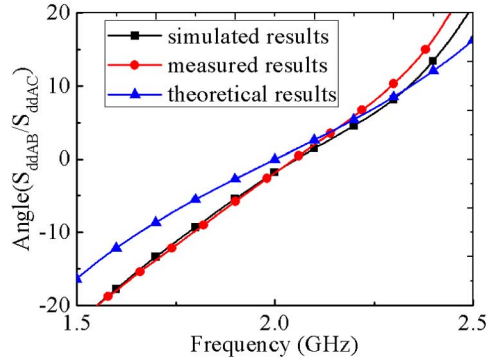

Fig. 7. Theoretical, simulated, and measured phase difference between balanced port B and C of the proposed balanced-to-balanced power divider prototype with power division ratio of 1:3[2].

The same rules as those in Section III-D are used to determine the bandwidths for measured and simulated results. The theoretical, simulated, and measured BW.S are 1.77–2.23, 1.71–2.13, and 1.74–2.10 GHz.

The theoretical, simulated, and measured phase differences of the two balanced ports are plotted in Fig. 7. The theoretical, simulated, and measured BW.P are 1.66–2.34, 1.78–2.34, and 1.79–2.29 GHz.

We define the frequency range that BW.S and BW.P overlap as the operating band. An operating band from 1.78 to 2.13 GHz is achieved in simulations with the FBW of about 17.5%. The measured operating band is from 1.79 to 2.10 GHz with the FBW of about 15.5%. Both of them are narrower than the theoretical value of 23% due to the tolerances of practical distributed circuit and fabrication.

V. Conclusion

In this paper, a two-way balanced-to-balanced power divider with arbitrary power division has been proposed and analyzed. The constraint rules of its single-ended S-parameters are first presented, which are obtained from the mixed-mode S-parameters. A balanced-to-balanced power divider with arbitrary power division is then built up with a combination of ideal transmission lines of different characteristic impedances loaded with specific resistances. Design equations are derived analytically to determine the critical parameters according to the desired power division ratio. The limitation and freedom for design are discussed in detail. The maximum power division ratio is 1:4.69[2] when the realizable characteristic impedance of transmission line is within 20–120 Ω. The FBW of our balanced-to-balanced power divider is further explored numerically. A prototype is realized by microstrip lines and two surface-mounted resistors. Good agreement is between the simulated and measured mixed-mode S-parameters to validate our design method. The balanced-to-

balanced power divider with arbitrary power division can be utilized in fully balanced RF front-ends with more flexibility.

REFERENCES

[1] D. M. Pozar, *Microwave Engineering*, 3rd ed. New York, NY, USA: Wiley, 2005, ch. 7.

[2] J.-S. Lim, S.-W. Lee, C.-S. Kim, J.-S. Park, D. Ahn, and S. Nam, "A 4:1 unequal Wilkinson power divider," *IEEE Microw. Wireless Compon. Lett.*, vol. 11, no. 3, pp. 124–126, Mar. 2001.

[3] Y.-J. Ko, J.-Y. Park, and J.-U. Bu, "Fully integrated unequal Wilkinson power divider with EBG CPW," *IEEE Microw. Wireless Compon. Lett.*, vol. 13, no. 7, pp. 276–278, Jul. 2003.

[4] L. Chiu and Q. Xue, "A parallel-strip ring power divider with high isolation and arbitrary power-dividing ratio," *IEEE Trans. Microw. Theory Techn.*, vol. 55, no. 11, pp. 2419–2426, Nov. 2007.

[5] J.-X. Chen and Q. Xue, "Novel 5:1 unequal Wilkinson power divider using offset double-sided parallel-strip lines," *IEEE Microw. Wireless Compon. Lett.*, vol. 17, no. 3, pp. 175–177, Mar. 2007.

[6] B. Li, X. Wu, and W. Wu, "A 10:1 unequal Wilkinson power divider using coupled lines with two shorts," *IEEE Microw. Wireless Compon. Lett.*, vol. 19, no. 12, pp. 789–791, Dec. 2009.

[7] J.-L. Li and B.-Z. Wang, "Novel design of Wilkinson power dividers with arbitrary power division ratios," *IEEE Trans. Ind. Electron.*, vol. 58, no. 6, pp. 2541–2546, Jun. 2011.

[8] K.-K. M. Cheng and P.-W. Li, "A novel power-divider design with unequal power-dividing ratio and simple layout," *IEEE Trans. Microw. Theory Techn.*, vol. 57, no. 6, pp. 1589–1594, Jun. 2009.

[9] H. Oraizi and A.-R. Sharifi, "Design and optimization of broadband asymmetrical multisection Wilkinson power divider," *IEEE Trans. Microw. Theory Techn.*, vol. 54, no. 5, pp. 2220–2231, May 2006.

[10] H. Oraizi and A.-R. Sharifi, "Optimum design of asymmetrical multisection two-way power dividers with arbitrary power division and impedance matching," *IEEE Trans. Microw. Theory Techn.*, vol. 59, no. 6, pp. 1478–1490, Jun. 2011.

[11] F. Lin, Q.-X. Chu, Z. Gong, and Z. Lin, "Compact broadband Gysel power divider with arbitrary power-dividing ratio using microstrip/slotline phase inverter," *IEEE Trans. Microw. Theory Techn.*, vol. 60, no. 5, pp. 1226–1234, May 2012.

[12] Y.-L. Wu, Y.-A. Liu, and S.-L. Li, "A modified Gysel power divider of arbitrary power ratio and real terminated impedances," *IEEE Trans. Microw. Theory Techn.*, vol. 21, no. 11, pp. 601–603, Nov. 2011.

[13] J.-C. Kao, Z.-M. Tsai, K.-Y. Lin, and H. Wang, "A modified Wilkinson power divider with isolation bandwidth improvement," *IEEE Trans. Microw. Theory Techn.*, vol. 60, no. 9, pp. 2768–2780, Sep. 2012.

[14] P.-H. Deng and L.-C. Dai, "Unequal Wilkinson power dividers with favorable selectivity and high-isolation using coupled-line filter transformers," *IEEE Trans. Microw. Theory Techn.*, vol. 60, no. 6, pp. 1520–1529, Jun. 2012.

[15] Y.-L. Wu, H. Zhou, Y.-X. Zhang, and Y.-A. Liu, "An unequal Wilkinson power divider for a frequency and its first harmonic," *IEEE Microw. Wireless Compon. Lett.*, vol. 18, no. 11, pp. 737–739, Nov. 2008.

[16] S.-H. Ahn, J.-W. Lee, C.-S. Cho, and T.-K. Lee, "A dual-band unequal Wilkinson power divider with arbitrary frequency ratios," *IEEE Microw. Wireless Compon. Lett.*, vol. 19, no. 12, pp. 783–785, Dec. 2009.

[17] Y.-L. Wu, Y.-A. Liu, Y.-X. Zhang, J.-C. Gao, and H. Zhou, "A dual band unequal Wilkinson power divider without reactive components," *IEEE Trans. Microw. Theory Techn.*, vol. 57, no. 1, pp. 216–222, Jan. 2009.

[18] Y.-L. Wu, Y.-A. Liu, Q. Xue, S. Li, and C. Yu, "Analytical design method of multiway dual-band planar power dividers with arbitrary power division," *IEEE Trans. Microw. Theory Techn.*, vol. 58, no. 12, pp. 3832–3841, Dec. 2010.

[19] Z.-Y. Sun, L.-J. Zhang, Y.-P. Yan, and H.-W. Yang, "Design of unequal dual-band Gysel power divider with arbitrary termination resistance," *IEEE Trans. Microw. Theory Techn.*, vol. 59, no. 8, pp. 1955–1962, Aug. 2011.

[20] H.-L. Zhang, B.-J. Hu, and X.-Y. Zhang, "Compact equal and unequal dual-frequency power dividers based on composite right-/left-handed transmission lines," *IEEE Trans. Ind. Electron.*, vol. 59, no. 9, pp. 3464–3472, Sep. 2012.

[21] J. W. May and G. M. Rebeiz, "A 40–50-GHz SiGe 1:8 differential power divider using shielded broadside-coupled striplines," *IEEE Trans. Microw. Theory Techn.*, vol. 56, no. 7, pp. 1575–1581, Jul. 2008.

[22] L.-S. Wu, B. Xia, and J. F. Mao, "A half-mode substrate integrated waveguide ring for two-way power division of balanced circuit," *IEEE Microw. Wireless Compon. Lett.*, vol. 22, no. 7, pp. 333–335, Jul. 2012.

[23] B. Xia, L.-S. Wu, and J. F. Mao, "A new balanced-to-balanced power divider/combiner," *IEEE Trans. Microw. Theory Techn.*, vol. 60, no. 9, pp. 287–295, Sep. 2012.

[24] M.-J. Park, "Comments on 'A new balanced-to-balanced power divider/combiner'," *IEEE Trans. Microw. Theory Techn.*, vol. 61, no. 2, p. 1000, Feb. 2013.

[25] B. Xia, L.-S. Wu, and J. F. Mao, "Authors' reply," *IEEE Trans. Microw. Theory Techn.*, vol. 61, no. 2, pp. 1001–1003, Feb. 2013.

[26] B. Xia and J.-F. Mao, "A new dual-band balanced-to-balanced power divider," *Progr. Electromagn. Res. C*, vol. 37, pp. 53–66, Jan. 2013.

Bin Xia was born in 1976. He received the B.S. and M.S. degrees in electromagnetic fields and microwave technologies from the People's Liberation Army (PLA) University of Science and Technology, Nanjing, China, in 2000, and 2003, respectively, and is currently working toward the Ph.D. degree in electromagnetic fields and microwave technologies at Shanghai Jiao Tong University, Shanghai, China.

From May 2003 to November 2005, he was an Engineer with the Institute of the General Staff Communication Design, Shenyang, China. Since November 2005, he has been a Lecturer with Zhenjiang Watercraft College People's Liberation Army (PLA), Zhenjiang, China. He is a Reviewer for *Progress in Electromagnetics Research* (PIER).

Lin-Sheng Wu (S'09–M'10) was born in 1981. He received the B.S. degree in electronic and information engineering and M.S. and Ph.D. degrees in electromagnetic fields and microwave technologies from Shanghai Jiao Tong University (SJTU), Shanghai, China, in 2003, 2006 and 2010, respectively.

From August to November 2010, he was a Research Fellow with the Department of Electrical and Computer Engineering, National University of Singapore. From February 2010 to January 2012, he was a Post Doctor with SJTU. He is currently a Lecturer with the Key Laboratory of Ministry of Education of Design and Electromagnetic Compatibility of High Speed Electronic Systems, SJTU, where his current research interest is mainly focused on novel techniques for microwave integration and passive components. He has authored or coauthored over 50 technical papers.

Dr. Wu was a session co-chair of the Asia–Pacific Microwave Conference (APMC) and the IEEE Electrical Design of Advanced Packaging and Systems Symposium (EDAPS) in 2011. He has been a reviewer for several international journals, including three times for the IEEE publications.

Si-Wei Ren, photograph and biography not available at time of publication.

Jun-Fa Mao (M'92–SM'98–F'11) was born in 1965. He received the B.S. degree in radiation physics from the University of Science and Technology of National Defense, Shanghai, China, in 1985, the M.S. degree in experimental nuclear physics form the Shanghai Institute of Nuclear Research, Shanghai, China, in 1988, and the Ph.D. degree in electronic engineering from Shanghai Jiao Tong University, Shanghai, China, in 1992.

Since 1992, he has been a faculty member with Shanghai Jiao Tong University, where he is cur-

rently a Chair Professor and the Executive Dean of the School of Electronic, Information and Electrical Engineering. From 1994 to 1995, he was a Visiting Scholar with the Chinese University of Hong Kong, Hong Kong. From 1995 to 1996, he was a Postdoctoral Researcher with the University of California at Berkeley, Berkeley, CA, USA. He is a Chief Scientist of The National Basic Research Program (973 Program) of China, a Project Leader of the National Science Foundation for Creative Research Groups of China, a Cheung Kong Scholar of the Ministry of Education, China, and an Associate Director of the Microwave Society of China Institute of Electronics. He has authored or coauthored over 190 journal papers (including 70 IEEE journal papers) and 120 international conference papers. His research interests include the interconnect and package problem of integrated circuits and systems and analysis and design of microwave circuits.

Dr. Mao was the 2007–2009 chair of the IEEE Shanghai Section and the 2009–2011 chair of the IEEE Microwave Theory and Techniques Society (IEEE MTT-S) Shanghai Chapter. He was the recipient of the 2004 National Natural Science Award of China, the 2008 National Technology Invention Award of China, the Best Paper Award of the 2008 Symposium of APEMC in conjunction with the 19th International Symposium of Zurich EMC.